Program Digest, 2019 IEEE International Ultrasonics Symposium (IUS)
Glasgow, Scotland, October 6-9, 2019

Detection and characterisation of defects in highly scattering materials using ultrasonic arrays

Long Bai, Alexander Velichko, and Bruce W. Drinkwater
Department of Mechanical Engineering, University of Bristol, Bristol, BS8 1TR, United Kingdom
Email:lb13340@bristol.ac.uk

***Abstract*— Coarse grained materials are widely used in the power generation industry and their inspection is critical for the safe operation of nuclear power plants. Ultrasonic array imaging is an important non-destructive testing method which is capable of detecting and characterising defects in a component. However, the performance of ultrasonic inspection can be severely affected by the existence of grains in a polycrystalline material which cause ultrasonic attenuation and backscatter. In this paper, we aim to explore the effect of two important parameters, frequency and inspection depth, on the characterisation accuracy of small side-drilled holes through experiments. The average grain size of the Inconel specimen is 750µm, and 2mm holes (in diameter) are found to be detectable when the frequency does not exceed 2 MHz even at large distances from the array (*i.e.* 60mm). Moreover, it is shown that reliable sizing of these small holes is achievable using the scattering matrix.**

Keywords— ultrasonic array, non-destructive testing, grain noise, scattering matrix, defect characterisation

I. INTRODUCTION

Ultrasonic arrays are widely used in non-destructive testing (NDT) applications for detection and characterisation of defects [1]. When ultrasonic waves propagate in a medium, scattering happens at material discontinuities such as defects, and the scattered waves carry important information that is useful for detection, localisation, and characterisation of defects. For materials having a complex microstructure (*e.g.* large grains), the grain boundaries also cause wave scattering and the measured signal can be severely contaminated by such coherent noise, known as multiple scattering noise [2]. As a result, the performance of conventional ultrasonic NDT techniques including array imaging degrades for coarse grained materials, and inspection of highly scattering materials remains a challenge.

Efforts have been made to improve the inspection performance of ultrasonic testing with the development of signal processing and advanced imaging algorithms [3], [4]. A statistical modelling approach, based on recent progress in finite element modelling of wave scattering in polycrystalline materials [5], was proposed and shown to improve the detection and characterisation accuracy [6]. This method requires data simulated from multiple random realisations of the grain structure and uses this information in a Bayesian inversion framework [6]. Although higher frequencies normally result in better image resolution and hence, better defect characterisation capability, the usable frequency range is often limited for coarse grained materials because the level of grain scattering noise increases dramatically as the frequency increases.

The main aim of this paper is to study the defect characterisation problem experimentally based on a specimen which has a large average grain size (750µm) and contains small side-drilled holes (2mm). In particular, we use the scattering matrix [6] for characterisation and explore the influence of the key parameters including the inspection depth and frequency on the characterisation performance. Based on multiple measurement data containing the same defect and different grain noise, the scattering-matrix-based approach was shown to achieve accurate characterisation at moderate conditions (*e.g.* defects that are 20mm from the array at 1.5 MHz), but the characterisation performance was shown to deteriorate at larger inspection depths and/or higher frequencies due to the increased noise.

II. EXPERIMENTAL CONFIGURATION AND IMAGING RESULTS

The specimen studied in experiments is a polycrystalline steel (Inconel 600) block of dimensions 90 mm×90 mm×284 mm. The average grain size of the specimen is 750µm and the specimen has an isotropic material property at a macroscopic scale [4]. Four 2mm side-drilled holes (in diameter) are manufactured at depths of 20mm, 40mm, 60mm, and 80mm [labelled #1, #2, #3, and #4 in Fig. 1(a)] from the top surface. Two 1D linear array probes with centre frequencies 1 MHz and 2 MHz are used in experiments, and detailed array specifications are given in Table I. In Fig. 1(a), the array is used to measure the defect data (containing grain noise), and for a given x location, multiple measurements (15 for the 1 MHz array and 16 for the 2 MHz array) are taken at different y locations to obtain different realisations of grain noise.

Ultrasonic attenuation and velocity are two key physical quantities that affect the imaging quality and scattering matrix extraction (see Section III) [6]. Measurements from defect-free regions are needed in order to calculate their values, and Fig. 1(b) shows the experimental configuration adopted for this purpose (besides the shown array location, measurements are also taken at three different x locations indicated with arrows). Fig. 2(a) shows the measured A-scan signal averaged over all trasmitter-receiver pairs (this will give equivalent pulse-echo signal obtained with an unfocused monolithic transducer [6]) and all four probe locations for the 2 MHz array. Dividing the propagation distance (180mm) by the difference between the

This project has received funding from the Euratom research and training programme 2014-2018 under grant agreement No 755500.

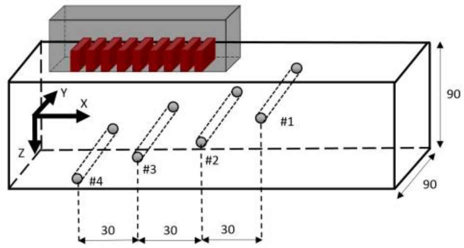

(a)

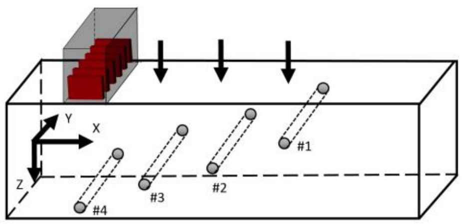

(b)

Fig. 1. Experimental configuration for (a) defect data measurement and (b) attenuation measurement.

TABLE I. ARRAY TRANSDUCER SPECIFICATIONS USED IN EXPERIMENTS

Array Label	Number of Elements	Central Frequency (MHz)	Element		
			Width (mm)	*Pitch (mm)*	*Length (mm)*
A	64	1	1.2	1.5	15
B	64	2	1.32	1.57	22

arrival times of the first and second backwall reflections gives the ultrasonic velocity of 5814m/s for the considered medium. The attenuation coefficient can be calculated from [6]

$$\alpha(\omega) = \frac{1}{2d} \ln \left| \frac{B_1(\omega)}{B_2(\omega)} \right|, \quad (1)$$

where $B_1(\omega)$ and $B_2(\omega)$ denote the spectra of the first and second backwall reflections [see Fig. 2(b)] and d (=90mm) is the depth of the specimen. The attenuation coefficient calculated using this approach is shown to be reliable in the frequency range between 0.9 MHz and 2 MHz [see Fig. 2(c)].

The TFM imaging algorithm [7] is applied to the experimental data and Fig. 3 shows results obtained at 1-3 MHz. The 2 MHz array is used to produce results at 2 MHz and 3 MHz by filtering the array data at the corresponding frequency, and filter bandwidth is 100% in all these cases. Figs. 3(a)-3(c) and Figs. 3(d)-3(f) correspond to data measured at two different y locations, 45mm (centre of the specimen) and 90mm (edge of the specimen), respectively, thus show different "noise realisations". It can be observed from these results that grain scattering noise increases as the frequency increases. For example, when the frequency is 3 MHz, the mean signal-to-noise ratio (SNR) of Hole 3 [located at (0, 60) mm] is only 14.9 dB with the standard deviation 2.1 dB [the noise RMS value is calculated from the 30mm×30mm noise region, shown as the red box in Fig. 3(c)]. As a result, the detection performance is expected to be poor, and image-based characterisation is also challenging at 3 MHz because the size of the defects (2mm) is

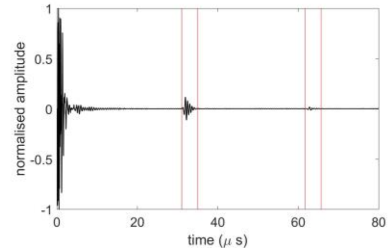

(a)

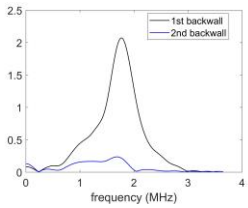

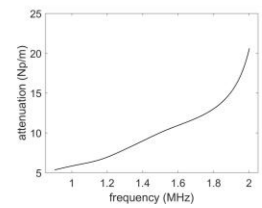

(b) (c)

Fig. 2. (a) Equivalent pulse-echo signal averaged over all tranmitter-receiver element pairs and probe locations. (b) Frequency spectra of the first and second backwall reflections. (c) Attenuation coefficient calculated using (1).

comparable to the wavelength (1.9mm). For this reason, we will explore using the scattering matrix for characterisation of these small defects at frequencies between 1-2 MHz in the next section.

III. DEFECT CHARACTERISATION USING THE SCATTERING MATRIX

Besides TFM imaging, an alternative approach to processing the full matrix of array data is to extract the scattering matrix of a defect, defined as [6]

$$S(\theta_{in}, \theta_{sc}, \omega) = \frac{a_{sc}(\omega)}{a_{in}(\omega)} \sqrt{\frac{d_{sc}}{\omega}} \exp\left[-\frac{i\omega d_{sc}}{c} + \alpha(\omega) d_{sc} \right]. \quad (2)$$

In the above equation, θ_{in}, θ_{sc} denote the incident and scattering angles, a_{in}, a_{sc} are the amplitude of the incident and scattering waves, d_{sc} refers to the (far-field) distance between the defect and the receiver element, and α is the frequency-dependent attenuation coefficient [Fig. 2(c)]. Figs. 4-5 show scattering matrices (extracted from the experimental data using the sub-array imaging approach [8]) of Holes 1 and 3 measured at two different y locations, 45mm (top rows) and 90mm (bottom rows), and for frequencies 1-2 MHz. It can be seen from these results that the effect of grain noise is significantly different for Holes 1 and 3 due to the difference in the inspection depth. The scattering matrices of Hole 1 still exhibit patterns similar to those of ideal side-drilled holes, *i.e.*, the amplitude is a constant in all diagonal lines. On the other hand, the scattering matrices of Hole 3 show anti-diagonal patterns which resemble crack-like defects [8]. In order to investigate the effect of grain noise on characterisation, we calculate the L2 distance defined in (3) [9] (N is the number of incident/scattering angles) between the experimentally measured scattering matrices and those of the reference defects, including cracks and holes of sizes 0.5-6 mm.

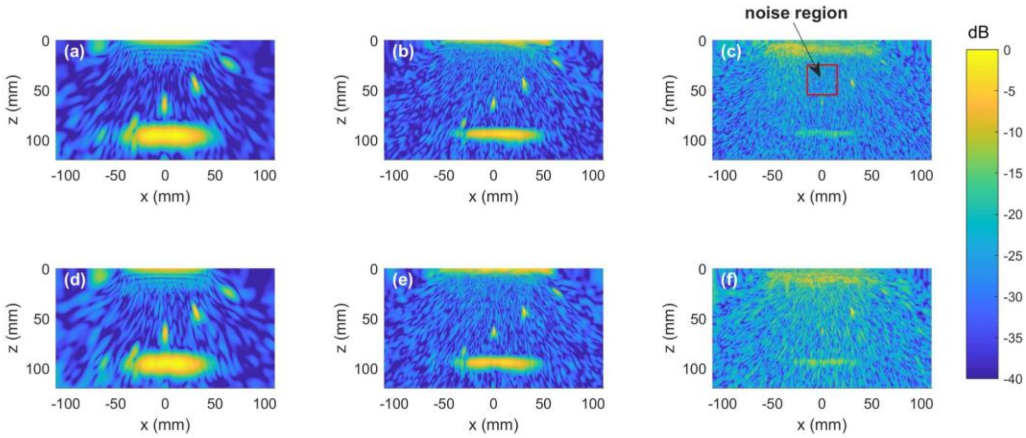

Fig. 3 TFM results obtained at y=45mm (a-c, centre of the specimen) and y=90mm (d-f, edge of the specimen) and at 1 MHz (a, d), 2 MHz (b, e) and 3 MHz (c, f). Measurement configuration is shown in Fig. 1(a).

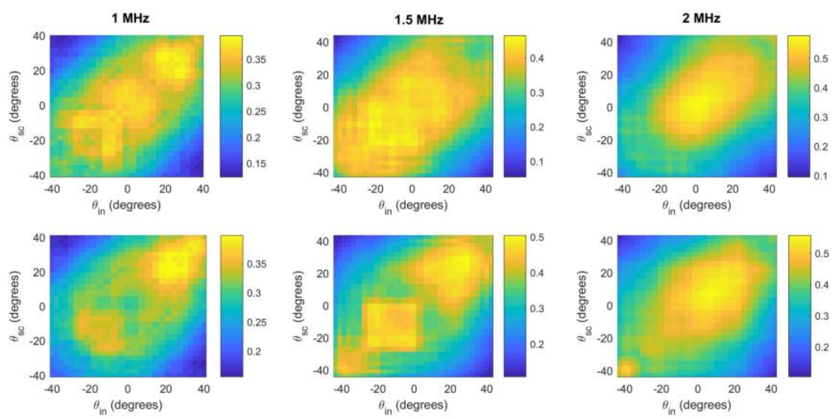

Fig. 4 The scattering matrix of Hole 1 measured at y=45mm (top row) and y=90mm (bottom row) at 1-2 MHz. The array centre is aligned with Hole 1 when performing the experiments.

$$\|S_1 - S_2\|_2 = \sqrt{\sum_{i=1}^{N}\sum_{j=1}^{N}[S_1(i,j) - S_2(i,j)]^2}. \qquad (3)$$

Figure 6 shows the mean L2 distance between the experimental measurements obtained at multiple y locations and the reference scattering matrices, and error bars correspond to the standard deviation. Under the nearest neighbour criterion, an experimentally measured scattering matrix can be identified to be measured from the reference defect with the smallest distance value. It can be seen that the L2 distance of 2mm hole is significantly smaller than the other defects at 1.5 MHz for Hole 1 (the top row), suggesting that accurate characterisation is possible. However, we also find for Hole 1 that there is uncertainty in the defect type at 1 MHz (*i.e.* the L2 distance of 2mm cracks is similar to that of 2mm holes) and uncertainty in size at 2 MHz (*i.e.* the L2 distance of 3mm holes is comparable to that of 2mm holes). Using the L2 distance metric, the defect type of Hole 3 is typically classified as a crack (see the bottom row in Fig. 6), but accurate sizing is still achievable at 1 MHz.

IV. Conclusions and Future Work

The performance of scattering-matrix-based defect characterisation has been shown through experiments to be reliable at relatively low frequencies. However, defect characterisation becomes more challenging as the inspection distance increases because of the higher grain noise level. It is noted that the results presented in this paper can potentially be improved by accurate modelling of defect and grain noise data distribution (*e.g.* through finite element simulations or repeated experiments from many specimens) and using this statistical information in inversion. Future work will aim to study the performance of the proposed approach for specimens having more complex defect types (*e.g.* branched cracks, surface-breaking cracks or porosity) and grain structures (*e.g.* materials with elongated grains).

Acknowledgment

We would like to thank Andreas Schumm, Antoine Ferré, and Pierre-Emile Lhuillier from EDF (EDF R&D, avenue des Renardières) for providing the mockup specimen.

References

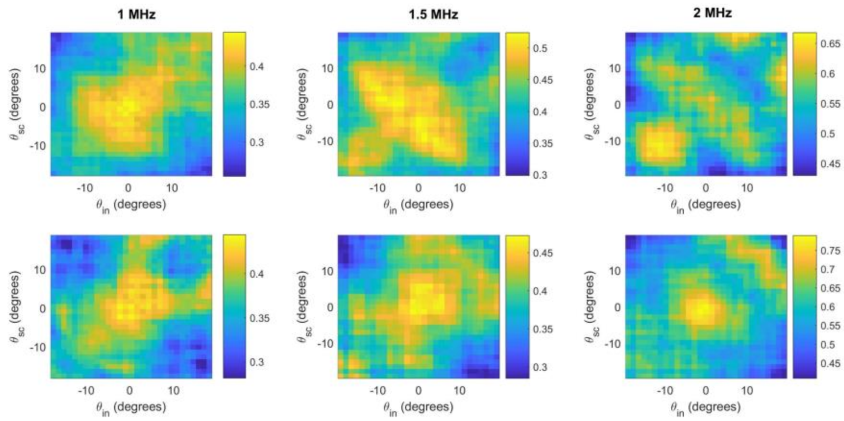

Fig. 5 The scattering matrix of Hole 3 measured at *y*=45mm (top row) and *y*=90mm (bottom row) at 1-2 MHz. The array centre is aligned with Hole 3 when performing the experiments [see Fig. 1(a)].

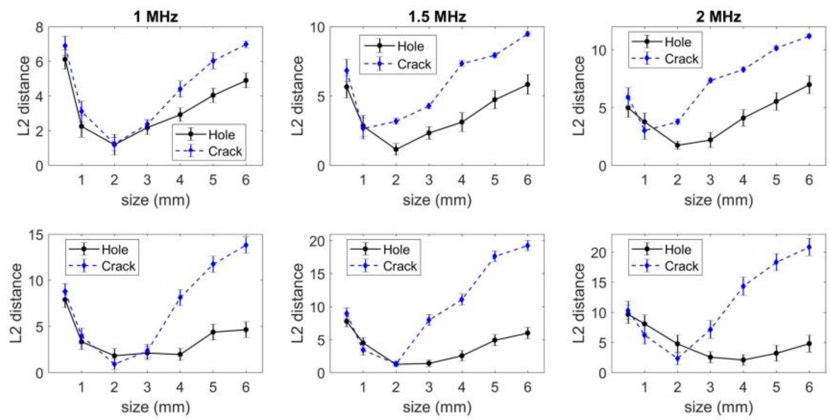

Fig. 6 The L2 distance [see (3)] between the reference scattering matrices and the experimentally measured scattering matrices of Hole 1 (top row) and Hole 3 (bottom row).

[1] B. W. Drinkwater and P. D. Wilcox, "Ultrasonic arrays for non-destructive evaluation: A review," NDT E Int., vol. 39, no. 7, pp. 525–541, 2006.

[2] A. Aubry and A. Derode, "Detection and imaging in a random medium: A matrix method to overcome multiple scattering and aberration," J. Appl. Phys., vol. 106, no. 4, p. 044903, 2009.

[3] A. Praveen, K. Vijayarekha, S. T. Abraham, and B. Venkatraman, "Signal quality enhancement using higher order wavelets for ultrasonic TOFD signals from austenitic stainless steel welds," Ultrasonics, vol. 53, no. 7, pp. 1288–1292, 2013.

[4] S. Shahjahan, A. Aubry, F. Rupin, B. Chassignole, and A. Derode, "A random matrix approach to detect defects in a strongly scattering polycrystal: How the memory effect can help overcome multiple scattering," Appl. Phys. Lett., vol. 104, no. 23, p. 234105, 2014.

[5] A. Van Pamel, C. R. Brett, P. Huthwaite, and M. J. Lowe, "Finite element modelling of elastic wave scattering within a polycrystalline material in two and three dimensions," J. Acoust. Soc. Am., vol. 138, no. 4, pp. 2326–2336, 2015.

[6] L. Bai, A. Velichko and B. W. Drinkwater, "Grain scattering noise modelling and its use in the detection and characterisation of defects using ultrasonic arrays," IEEE Trans. Ultrason. Ferroelectr. Freq. Control, in press.

[7] C. Holmes, B. W. Drinkwater and P. D. Wilcox, "Post-processing of the full matrix of ultrasonic transmit-receive array data for nondestructive evaluation," NDT E Int., vol. 38, no. 8, pp. 701–711, 2005.

[8] J. Zhang, B. W. Drinkwater and P. D. Wilcox, "Defect characterization using an ultrasonic array to measure the scattering coefficient matrix," IEEE Trans. Ultrason. Ferroelectr. Freq. Control, vol. 55, no. 10, pp. 2254–2265, 2008.

[9] A. A. Goshtasby, Image Registration: Principles, Tools and Methods. London, UK: Springer-Verlag, 2012